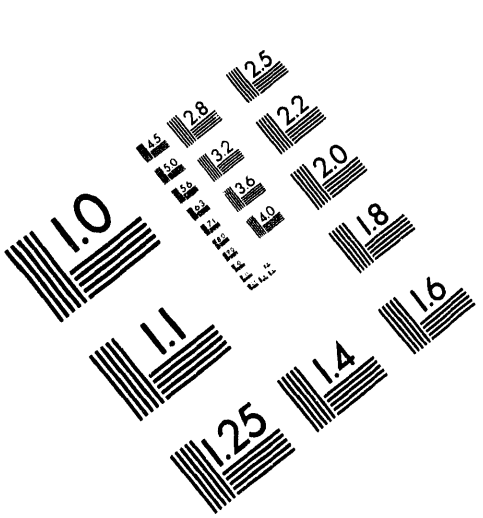

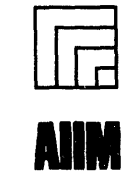

Association for Information and Image Management
1100 Wayne Avenue, Suite 1100
Silver Spring, Maryland 20910
301/587-8202

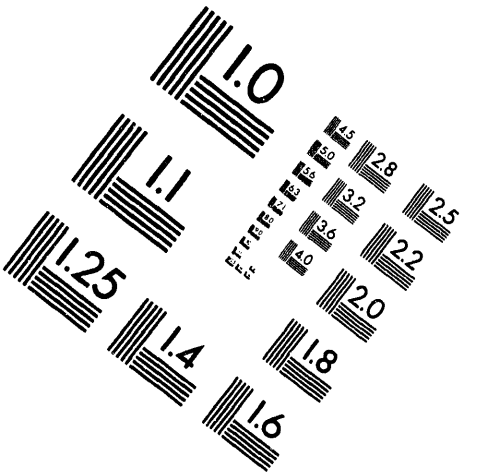

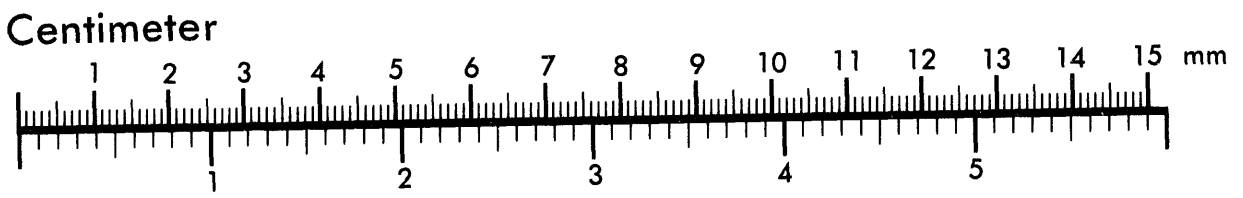

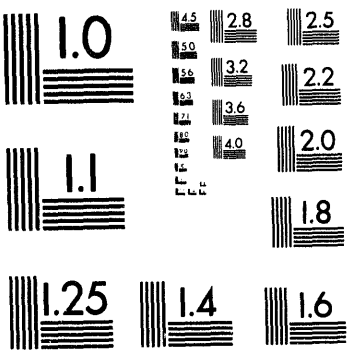

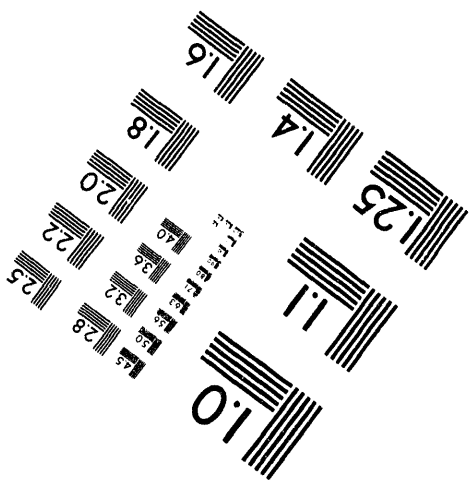

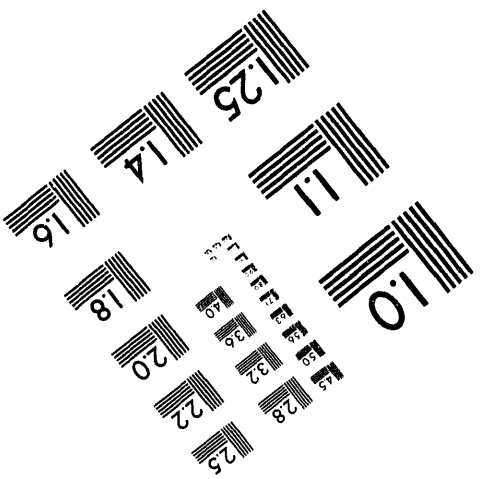

1 of 1

LBL-35318
UC-400

Some Effects of Heat Release in Premixed Flames

I.G. Shepherd

Combustion Group
Energy and Environment Division
Lawrence Berkeley Laboratory
University of California
Berkeley, California 94720

March 1994

This work was supported by the Director, Office of Energy Research, Office of Basic Energy Sciences, Chemical Sciences Division, of the U.S. Department of Energy under Contract No. DE-AC03-76SF00098.

Abstract

Numerical and experimental results are presented to illustrate some hydrodynamic effects of heat release in premixed flames. The heat release is represented by a simple model which treats the flame front as a two dimensional line source of volume. The velocity and strain rate induced in the flow field are determined and the numerical solution for the case of a laminar double kernel ignition is obtained. Of primary interest is the strain induced in the reactants between the expanding flame kernels and, for heat release rates typical of hydrocarbon flames, the strain rate at the plane of symmetry midway between the kernels upto 150 s^{-1}. The effects of kernel size, density ratio across the flame front and laminar burning velocity are studied.

For the case of turbulent combustion the velocity induced in the reactant stream is measured in a plane parallel to the flame holder of an open premixed turbulent v-shaped flame. A divergent flow field, with a strain rate of 50 s^{-1}, is induced by the heat release in the flame zone and the consequences of this for determining the turbulent burning velocity in this and similar systems is reviewed.

Introduction:

The flamelet concept has proved very fruitful as a means to understand the behavior of premixed turbulent flames at high Damköhler and Reynolds numbers. These flame zones are considered to consist of strained premixed laminar flame fronts which are stretched and wrinkled by the local turbulent flow field. The flame fronts separate regions of uniform composition: reactants and products. The burning velocity is then determined from the local structure of the laminar flamelets: the local curvature, flow divergence and Lewis number.

Over a range of time and length scales it is often possible to treat the flame as a zero thickness interface and many models and analysis strategies have taken advantage of this fact. With straightforward tomographic techniques it is possible to delineate the instantaneous flame front position and analyze the resulting data by fractal [1] and spectral [2] techniques. The geometry of the flame interface may also be described in terms of flame front curvature or flame orientation. These data may then used to characterize the flamelets in terms of distributions of local burning rates and flame front surface areas. The flamelet idea is also useful in theoretical and numerical investigations of premixed turbulent flames. Models based on this concept have proved quite successful: the BML model [3] for the scalar field and the G equation formalism [4] amongst many others.

In this context the aspect of In premixed combustion systems the exothermicity of the flame as well as the flame front geometry must be modeled. A successful approach to this problem [5-8] is to treat the interface so that the heat release is modeled as a

volumetric expansion at the flame font. The flame is thus represented by a collection of sources in a flow at uniform density and pressure and it is assumed that the flow Mach number is small enough so that the flow is dynamically incompressible. This approach has been further improved by the inclusion of baroclinic vorticity production which is necessary to balance momentum across the flame front.

An important feature of the heat release is that it can modify the far field by inducing flow in the reactants and products. This aspect, with special emphasis on the induced strain field, will be addressed from various perspectives: the flow induced by a flame font segment; a numerical example of flow induced in the reactants; the affect of heat release in a turbulent premixed v-shaped flame. Shepherd and Kostiuk [9] have demonstrated recently that flow divergence in turbulent premixed flame zones can have a significant affect on the determination of the burning rate and this issue will also be discussed.

Flow induced by line sources:

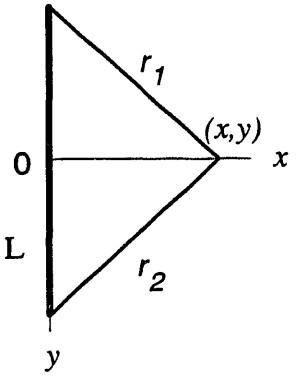

Figure 1

The flow field induced by a thin flame front may be illustrated by considering a two dimensional flame segment modeled as an array of sources. Figure 1 shows a flame sheet, 2L in width, aligned with the y axis, centered at x=0. This sheet is represented by line sources which are infinite in the out-of-plane direction. It can be easily shown [8] that the velocity induced parallel to the flame sheet, v, is

$$v = \frac{\tau S_L}{2\pi} \ln\left(\frac{r_1}{r_2}\right)$$

where r_1 and r_2 are the distances from the ends of the sheet to a point (x,y), S_L is the laminar burning velocity, and τ=R-1 is a heat release parameter (R is the density ratio across the flame).

$$r_1^2 = x^2 + (y+L)^2$$

$$r_2^2 = x^2 + (y-L)^2$$

$$v = \frac{\tau S_L}{4\pi} \ln\left(\frac{r_1^2}{r_2^2}\right)$$

At y=0 the velocity is zero due to symmetry. The strain rate, a, induced by the line source parallel to itself , dv/dy, is

$$\frac{dv}{dy} = a = \frac{\tau S_L}{2\pi}\left(\frac{y+L}{x^2+(y+L)^2} - \frac{y-L}{x^2+(y-L)^2}\right) \qquad (1)$$

Figure 2a shows the normalized strain rate induced parallel to the line source for increasing distance from the source at constant segment length and Fig. 2b shows the effect of segment length at constant x. Both these effects reduce the strain rate as can be seen from Equation (1). The induced strain at the x axis, y=0, is

$$a|_{y=0} = \frac{\tau S_L}{\pi}\left(\frac{L}{x^2 + L^2}\right) \qquad (2)$$

It is clear from this result that for a planar flame at large values of L the strain rate at the flame center will be negligibly small. In general, however, the induced flow at a point will be a function of the size and shape of the flame sheet. Substituting values characteristic of hydrocarbon flames, $\tau = 7$, $S_L = 45$ cm/s, $x = 1$ cm and $L = 2.5$ cm, gives a strain rate, at y = 0, of $a_t = 35\ s^{-1}$. Considering the overall velocity field it should be recalled that the flame segment is embedded in a flow is propagating into the reactant stream at S_L and that the resultant flame motion will also be affected by the boundary conditions of the flow. For example, when the burnt gas is at rest, as in an ignition from a point or line in a quiescent gas, the flame front will move with a radial velocity of RS_L.

Numerical Example: Double Kernel Ignition

An experimental method used to determine the burning velocity in laminar [10] and turbulent [11] premixed flames is the double kernel technique where two flames propagate towards each other from simultaneous point ignitions. As the flames approach they become planar and as the flow along the line joining the ignition sources stagnates it is assumed that their relative velocity in laboratory coordinates will tend towards twice the burning velocity. The results of two dimensional numerical simulation of this system are presented in this section. Emphasis is placed on the strain rate induced in the reactant flow by the expanding flame kernels

The algorithm used here is based on that developed by Ashurst [7] to model open v-shaped and Bunsen flames. This is a Lagrangian model which represents the flame front as a collection of point sources. The flow is two-dimensional and, as the velocities are small compared to the speed of sound, it is dynamically incompressible. The flame front propagates normal to itself at a fixed speed, S_L, by a Huygens mechanism and by the affect of volumetric expansion at all the other point sources. The affect of flame stretch on S_L is not considered and the baroclinic production of vorticity in the products was not included in the simulations.

The spacing between the point sources was 0.25 mm and the time step 0.1 msecs. At each time step the expanding flame front was fitted by a spline and redescretized at the constant node spacing. The coordinate system is defined so that the x axis (u velocity) joins the centers of the initial flame kernels and y (v velocity) is the orthogonal axis at the plane of symmetry between the ignition sources (the stagnation plane). Table 1 shows the conditions for the simulations performed where x_0 is the distance from the mid point

between the flame kernels to the center or the initial flame kernels and r_0 is the initial kernel radius.

Case	S_L (cm/sec)	R	r_0 (mm)	x_0 (mm)	a_m(s^{-1})	a_0 (s^{-1})
A	20	5.5	1.5	±10	100	30
B	30	6.5	1.5	±10	180	50
C	40	7.5	1.5	±10	280	60
D	40	7.5	3.0	±20	140	30
E	40	7.5	1.5	±6	470	150

Table I: Conditions for simulations

The algorithm was tested by simulating a single kernel ignition for condition C and determining the radial speed of the flame front. This was found to equal RS_L. Figure 3 shows the results of a simulation of a double kernel ignition in a quiescent gas for case A. Only the right hand side of the domain is calculated a symmetry condition being imposed by representing the 'mirror' flame as image sources of those on the first. The flame front was moved under the influence of the flow field produced by these two sets of sources and was propagated normal to itself at the laminar burning velocity. The position of the flame fronts is shown at equal time intervals as they propagate away from the 3 mm diameter ignition kernels. The volumetric expansion at the flame fronts produces a stagnation point at x=0 and, as the two kernels approach each other, the flame speed slows and the flame fronts become planar.

Figure 4 presents the position of the flame front, x_f at y=0 as it evolves with time for cases A, B and C (Table I) which have the same initial conditions of kernel size and location but have a range of laminar burning velocities and density ratios characteristic of hydrocarbon/air flames. As indicated above in the absence of a second flame kernel the flame speed will be RS_L and it is possible to compare these cases by normalizing the time by the heat release, $t^* = tRS_L/x_0$ and x_f by the initial position of the flame, $x^* = x_f/(x_0 - r_0)$. The flame motion starts to be significantly affected by the presence of the stagnation point when t^*>0.25 (x^*<0.75) and its velocity falls rapidly thereafter towards S_L. By the end of the simulation the speed of the flame front movement had fallen to within 30% of S_L. It will be observed that rate of velocity change is a function of the source strength, case C slowing the most.

Equation 1 shows that a strain field exists in the reactant gas parallel to the flame front. The induced velocity along the y axis where u=0 was also determined during the simulations and from a spline fit of the results the distribution of strain obtained. Figure 5 shows the distribution of strain along the y axis for cases A, B and C at a flame front separation of 2 mm. This profile is similar to that observed in Figures 2a,b. The evolution of the strain rate at the stagnation point as the flame approaches it is shown in figure 6 for these three cases. It has been normalized as indicated by equation 2 as, $a^* = ax_0/\tau S_L$.

The strain rate rises rapidly to reach a maximum, a_m (given in Table I) as the flame front motion begins to slow and then it falls as the flame front nears the stagnation point and becomes progressively more planar (see equation 2). The values of the strain rate when the flame front reaches the stagnation surface, a_0, obtained by second order extrapolation are given in Table I.

Figure 7 shows that the size of the flame kernel has a significant impact on the strain rate. The heat release rate is the same for these cases, C-E, but the initial separation of the flame kernels, $2x_0$, varies from 12 (E) to 40 mm (D). The maximum strain rates, from 470 (E) to 140 (D), scale with this separation. Figures 6 and 7 demonstrate that, although the strain rates scale in the expected ways, they are very dependent on the instantaneous flame shape and size, and also change continuously throughout the simulations. As the local burning velocity is a function of the local strain rate (the tangential velocity gradient) measurements of the laminar burning velocity by the double kernel method should be assessed for this affect. The flame shape and size will also affect the burning rate determined in the turbulent analog of this system to be discussed below.

Turbulent v-shaped flame:

Similar processes to those outlined above will clearly occur in turbulent flame zones where the flame fronts are thin and the flamelet concept is applicable. In a turbulent flame, although the total heat release can be much larger, it will be distributed over the flame zone. The of flame front orientation [12] will also be randomly distributed. These factors make the modeling the affects of heat release in such systems very complex An experimental study of the flow induced by heat release in a premixed turbulent v-shaped flame was, therefore performed.

A uniform axisymmetric flow of premixed methane/ air (stoichiometric ratio, ϕ=0.9) at an exit velocity of $5m/s$ is provided by a $50mm$ diameter nozzle. A coflowing air stream at the same velocity shields the inner flow from interaction with the room air. The reactant flow turbulence (7%), generated by a perforated plate $50mm$ upstream of the burner nozzle, has an integral length scale of $3mm$ and the turbulent Reynolds number, based on these values, is 70. A 2 mm diameter rod placed at the burner exit is the flame stabilizer. The experimental set up has been described in detail elsewhere[13]. The origin of the coordinate system is at the center of the flame holder: x and y are the coordinates in the axial and transverse directions respectively and the z coordinate is parallel to the flame holder.

Experiments were performed to measure the strain rates induced in the reactant stream tangential to the mean flame position at z=0 and also parallel to the flame holder. The position of the mean flame zone was determined by measuring the light scattered from an argon ion laser beam (probe volume diameter 250μm) by micron sized oil droplets seeded in the reactant stream which evaporate at the flame front. Measurements were performed along transverse traverses (z=0) which passed through the flame zone. From these results a map of the scalar field in terms of the mean progress variable, $\bar{c}$ (c=0 in the

reactants and 1 in the products) was obtained. Using this map conditioned axial and transverse velocities were obtained on a grid normal and tangential to the mean flame zone by LDV. The velocities were conditioned by seeding the flow with the oil droplets so that only measurements in the reactants were obtained. By a similar process the velocity component parallel to the flame holder was evaluated.

Figure 7 shows the velocities tangential to contours of mean progress variable, U_t, in the (x,y,0) plane from the axial positions x=28 to x=78 mm. The axial and transverse velocities at the particular $\bar{c}$ value were obtained by interpolation and then transformed to give the components normal and tangential to the $\bar{c}$ contour. The strain rate induced in the reactants by the heat release, a_{xy}, along the $\bar{c}$ contours is of interest here and so the distance along the contours, s, was determined and the strain rate was evaluated as $a_{xy} = dU_t/ds$. The a_{xy} values obtained by least mean square fits are also shown in figure 7. The strain rate is quite low and falls slightly with increasing $\bar{c}$ value.

The strain rate, a_z, induced in the approach flow in the direction parallel to the flame stabilizer rod was also measured. Figure 8 presents this velocity component, W, for a traverse along the line (56,30,z) at $\bar{c}$=0.05 The strain rate, at z=0, was found to be 48 s^{-1}. The value does not vary significantly with downstream distance: measurements along (28,12,z) for the same flame gave a strain rate of 49 s^{-1}. Figure 8 also shows that this open flame cannot be treated as a two dimensional system because of the significant flow divergence out of the (x,y) plane. It is also clear from these results that the conventional measure of the turbulent burning rate [12], the velocity component normal to the mean flame position, would be in error due to the flow divergence induced in the reactant stream by the volumetric expansion in the flame zone.

Shepherd and Kostiuk [9] have recently studied in some detail the problems associated with determining the burning rate of turbulent premixed flames propagating into diverging flows. Their analysis results in an equation relating the burning rate in a turbulent flame to the mass fluxes which in two dimensions is

$$-\bar{\rho}\tilde{u}_\xi\Big|_\zeta - \int_{-\infty}^{\zeta} \nabla_r(\bar{\rho}(1-\tilde{c})\tilde{u}_r)\,d\xi + \int_{\zeta}^{\infty} \nabla_r(\bar{\rho}\tilde{c}\tilde{u}_r)\,d\xi + \int_{-\infty}^{\infty} \nabla_r(\overline{\rho c'' u_r''})\,d\xi = \int_{-\infty}^{\infty} \bar{w}\,d\xi \qquad (3)$$

I II III IV

where ζ is some point on the coordinate normal to the mean flame zone ξ and r the coordinate perpendicular to ξ. The right hand side of equation 3 is the local reaction rate of the flame integrated through the flame zone and hence the overall burning rate. This is related to the mass flux (I) at a plane ζ and gradients of the transverse mean (II and III) and turbulent (IV) mass fluxes. Only in a one dimensional system when II-IV are zero can the burning rate be equated with the mass flux (I) and to a flow velocity. A full description of the derivation of equation 3 and its consequences is given in [9].

It has been shown for the case of an open v-shaped flame heat release can induce flow divergence in the reactants resulting in non-zero gradients terms in the mass fluxes which therefore must be included for a correct determination of the burning rate. It should also be noted that a small flow divergence does not necessarily imply that the correction to I would also be small as terms II-IV are integrated across the flame zone which can be quite thick. A large amount of data relating the turbulent burning velocity to turbulence parameters has been collected by Bradley [11] from experiments based on the turbulent analog of the double kernel ignition experiment analyzed above. In the light of the present results it is probable that heat release induced flow divergence occurs in that system and the results should be reviewed, if possible, to determine whether this is a significant factor or not.

Conclusions:

A numerical and experimental study has been performed to assess the impact of heat release on premixed flames.

The heat release at the flame front has been modeled by treating the flame as a collection of volume sources. A double kernel ignition was numerically simulated and the flow induced in the reactants between the expanding kernels was studied with special emphasis on the strain rate along the axis of symmetry. This was found to be sensitive to the size and shape of the flame front which indicates that care must be taken when interpreting experimental measurements of the burning velocity by this method.

Experiments were performed in a turbulent premixed v-shaped flame and the strain rates in the approach flow were determined tangential to the mean flame position normal to the plane of the flame and parallel to the flame stabilizer rod. Flow divergence in the reactant stream was observed and the significance of this for conventional measurements of the turbulent burning rate were assessed. The neglect of this heat release induced flow divergence can lead to significant errors.

Acknowledgments

This work was supported by the Director, Office of Energy Research, Office of Basic Energy Sciences, Chemical Sciences Division of the U. S. Department of Energy under Contract No. DE-AC-03-76SF00098. The author is grateful for some of the numerical software and advice to Wm.T.Ashurst, help with the experiments from R.K.Cheng and discussions with F.Gouldin and L.Kostiuk.

References:

1. Shepherd, I.G., Cheng, R.K. and Talbot, T., *Exp in Fluids*, **13**, 386-392, 1992

2. Wirth, M. and Peters, N., *24th. International Combustion Symposium*, 493-501, 1992

3. Bray, K.N.C. *Springer Series in Chemical Physics*, **47**, 356, 1987

4. Kerstein, A.R., Ashurst, Wm.T. and Willuams, F.A., *Phys. Rev.*, **A37**, 2728, 1988

5. Ghoneim, A.F., Chorin, A.J. and Oppenheim, A.K., *Phil. Trans. R. Soc.*, **A394**, 303-325, 1982

6. Sethian, J.A., *J. Comp. Phys.*, **54**, 425-456, 1984

7. Ashurst, Wm.T., *Comb. Sci. and Tech.*, **52**, 325-351, 1987

8. Pindera, M.Z., *Ph.D. Thesis*, U.C. Berkeley, 1986

9. Shepherd, I.G. and Kostiuk, L.W., *Comb. and Flame*, **96**, 371-380, 1994

10. Raezer, S.D. and Olsen, H.L., *Comb. and Flame*, **6**, 227, 1962

11. Bradley, D., *24th. International Combustion Symposium*, 247-262, 1992

12. Shepherd, I.G. and Ashurst, Wm.T., *24th. International Combustion Symposium*, 485-491, 1992

13. Cheng, R.K. and Ng, T., *Comb. and Flame*, **57**, 155, 1984

Figure Captions:

Figure 2a: Strain rate induced by a line source: the affect of distance from the source.

Figure 2b: Strain rate induced by a line source: The effect of source strength

Figure 3: Time history of an ignition simulation: $S_L = 20$ cm/s, $\tau = 4.5$.

Figure 4: Flame front motion approaching the stagnation plane

Figure 5: The distribution of strain rate along the stagnation plane, $x = 0$.

Figure 6: Strain rate at $y = 0$ during simulations for cases A-C

Figure 7: The effect of kernel size on strain rate, $y = 0$.

Figure 8: The starin rate measured tangential to a v-shaped turbulent flame, $z = 0$.

Figure 9: Heat release induced flow divergence parallel to the flame holder: $x = 56$, $y = 30$

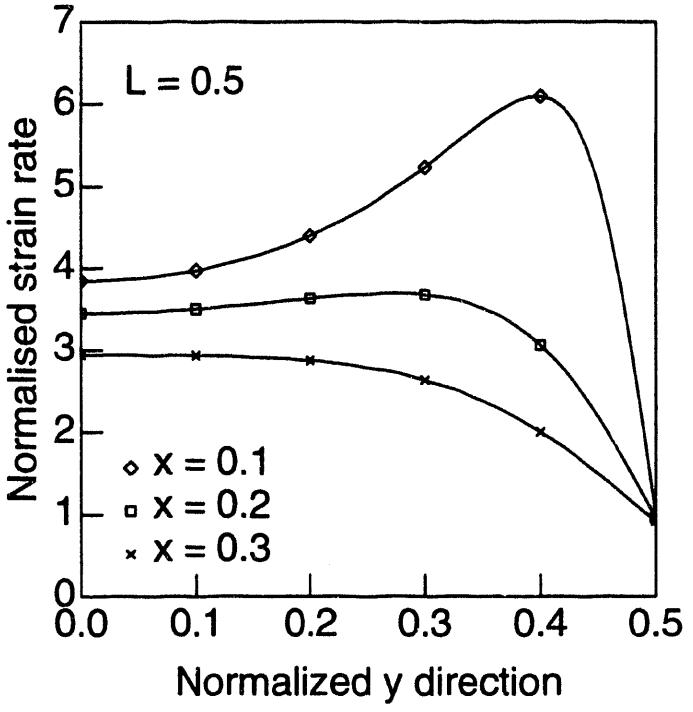
L = 0.5
x = 0.1
x = 0.2
x = 0.3
Normalised strain rate
Normalized y direction
0
1
2
3
4
5
6
7
0.0
0.1
0.2
0.3
0.4
0.5

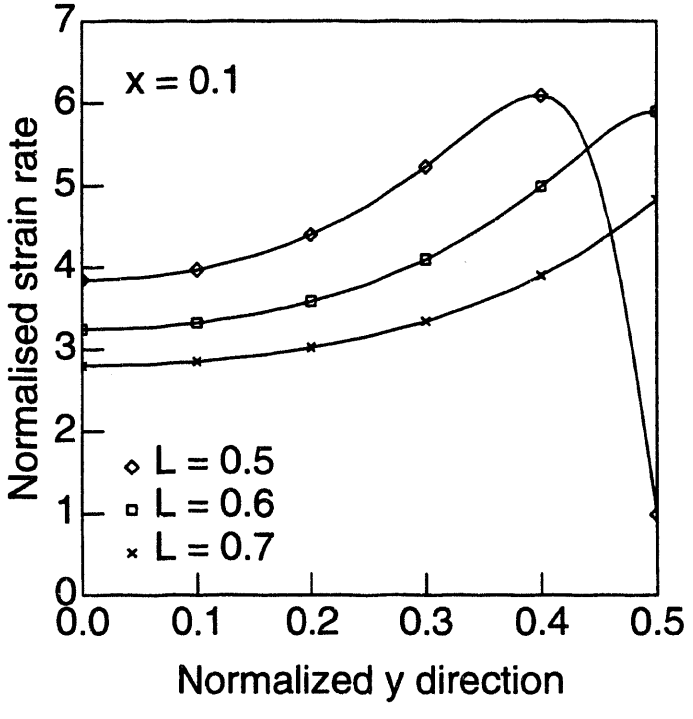
x = 0.1
L = 0.5
L = 0.6
L = 0.7
Normalised strain rate
Normalized y direction
0
1
2
3
4
5
6
7
0.0
0.1
0.2
0.3
0.4
0.5

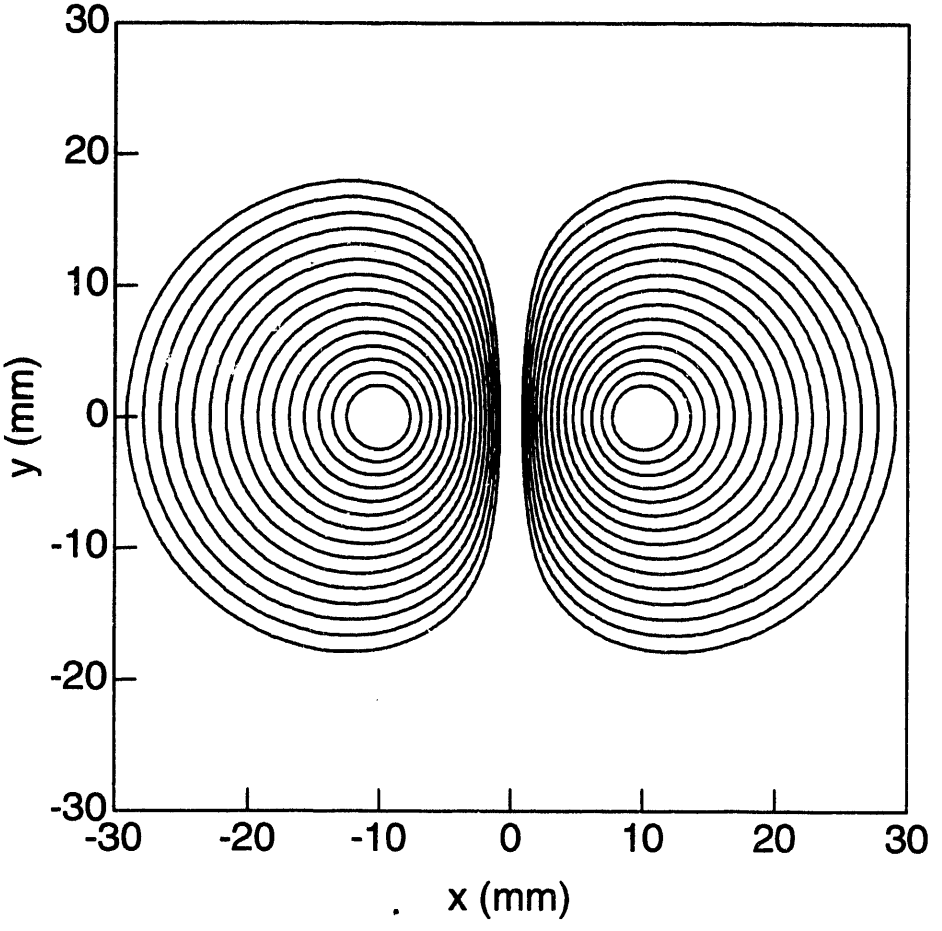
30
20
10
0
-10
-20
-30
y (mm)
-30
-20
-10
0
10
20
30
x (mm)

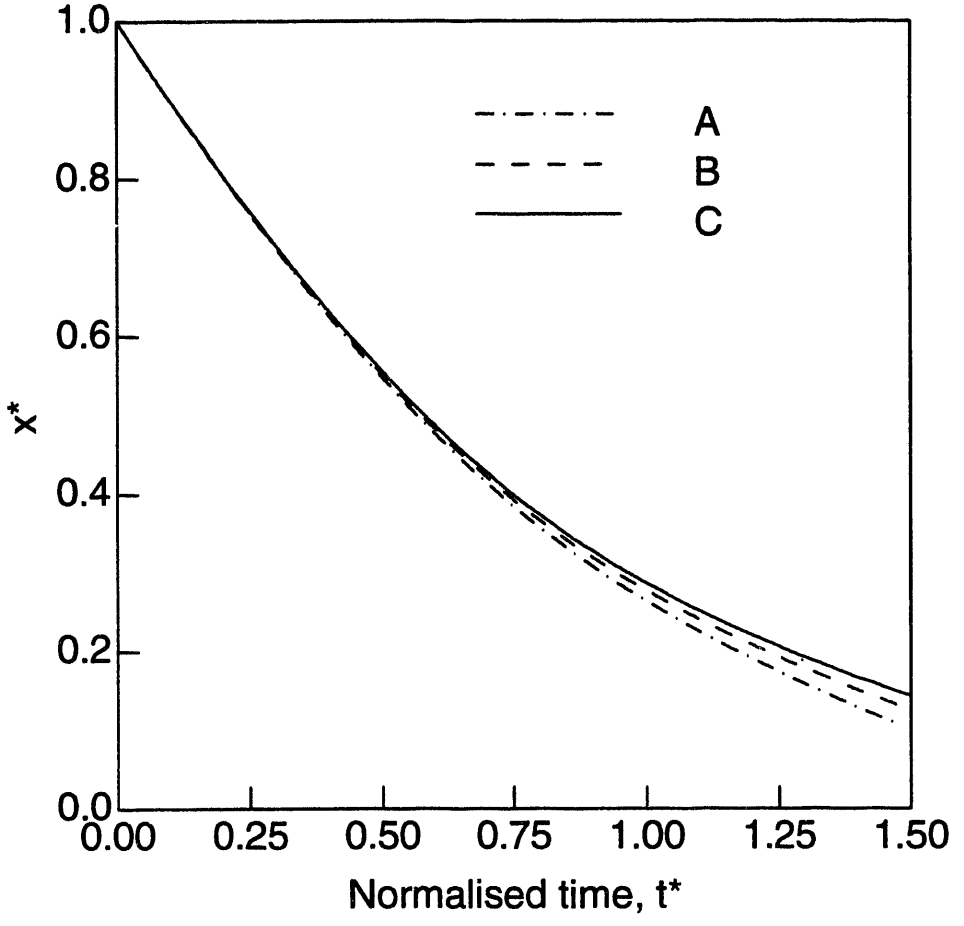
1.0
0.8
0.6
0.4
0.2
0.0
x*
0.00
0.25
0.50
0.75
1.00
1.25
1.50
Normalised time, t*
A
B
C

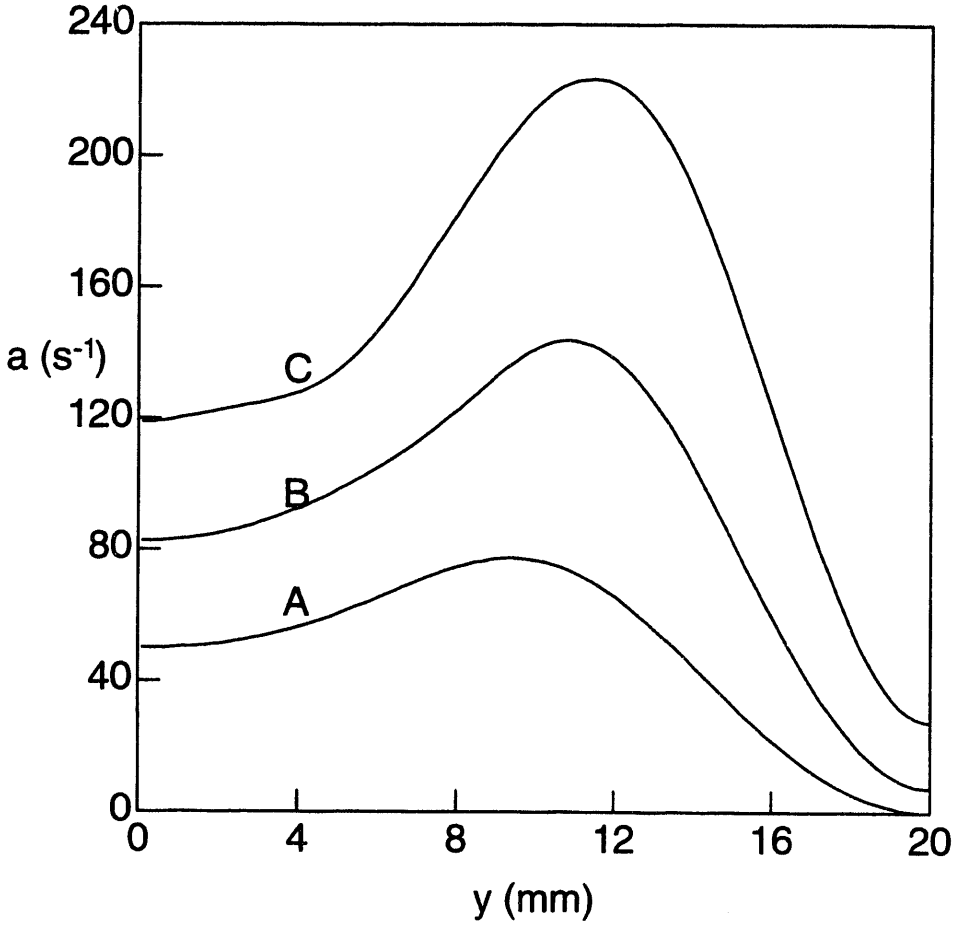
240
200
160
120
80
40
0
a (s-1)
C
B
A
0
4
8
12
16
20
y (mm)

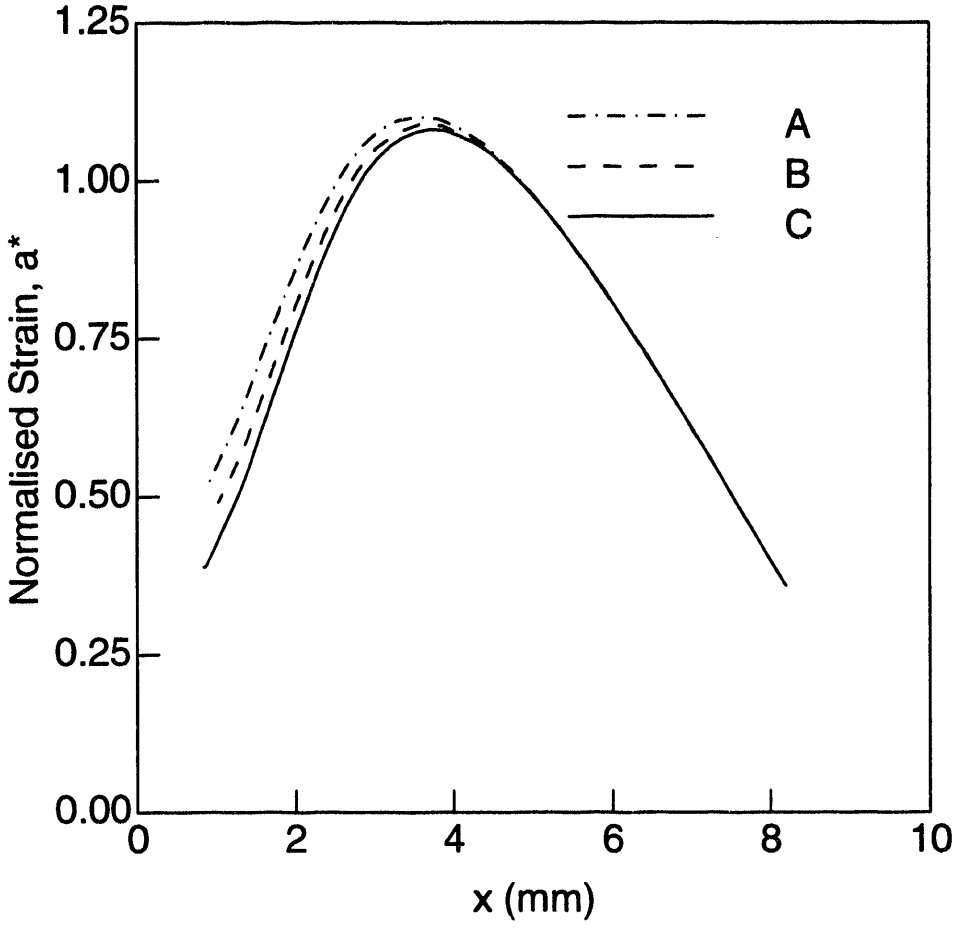
1.25
1.00
0.75
0.50
0.25
0.00
Normalised Strain, a*
0
2
4
6
8
10
x (mm)
A
B
C

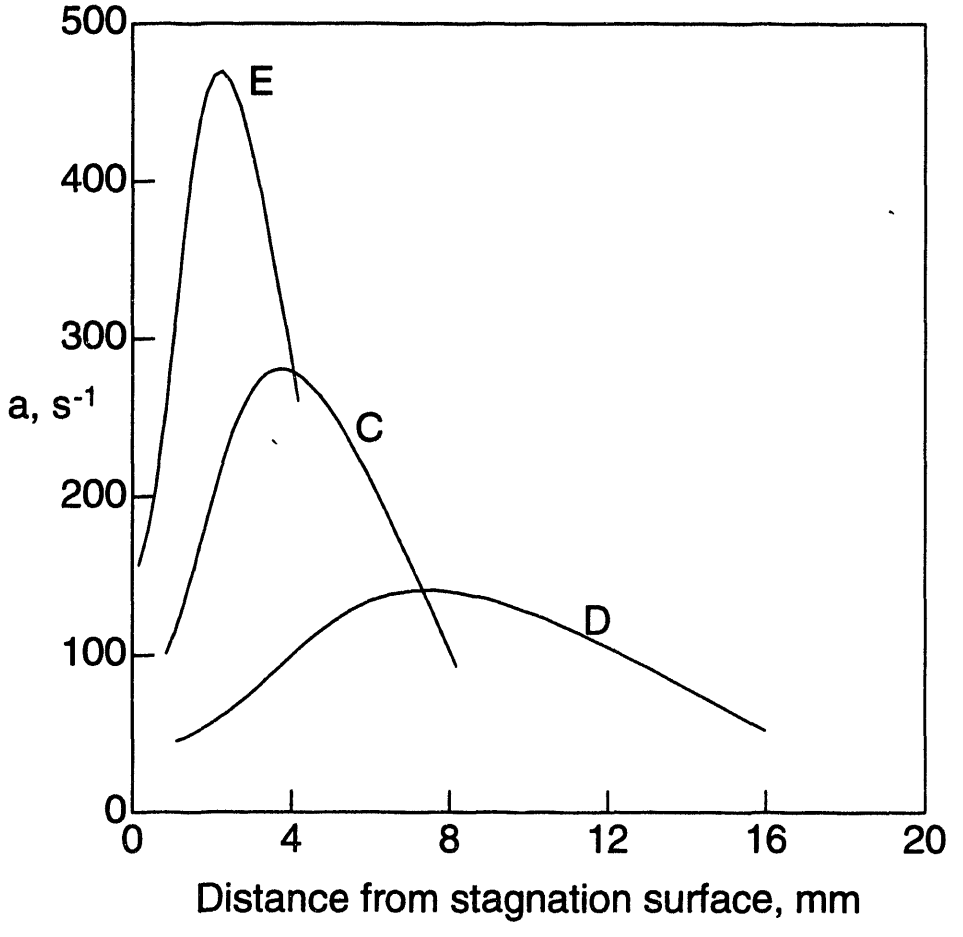
500
400
300
200
100
0
a, s-1
E
C
D
0
4
8
12
16
20
Distance from stagnation surface, mm

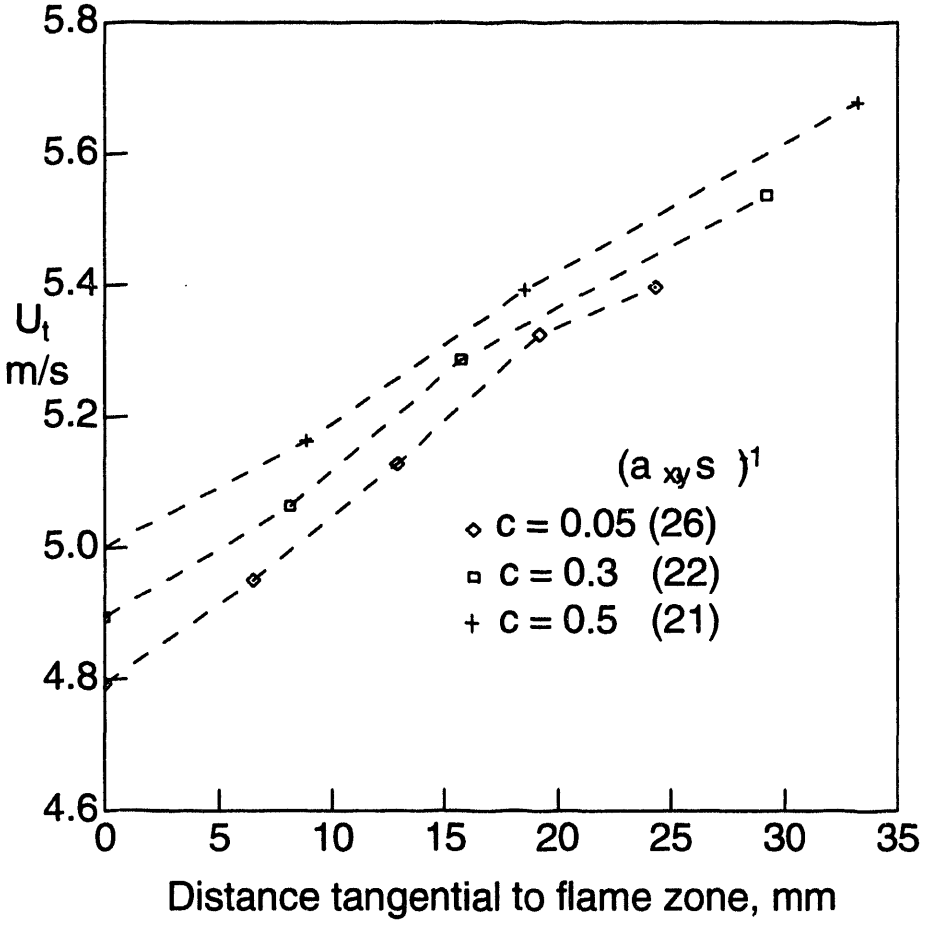
5.8
5.6
5.4
U_t
m/s
5.2
5.0
4.8
4.6
0
5
10
15
20
25
30
35
$(a_{xy}s)^1$
◇ c = 0.05 (26)
▫ c = 0.3 (22)
+ c = 0.5 (21)
Distance tangential to flame zone, mm

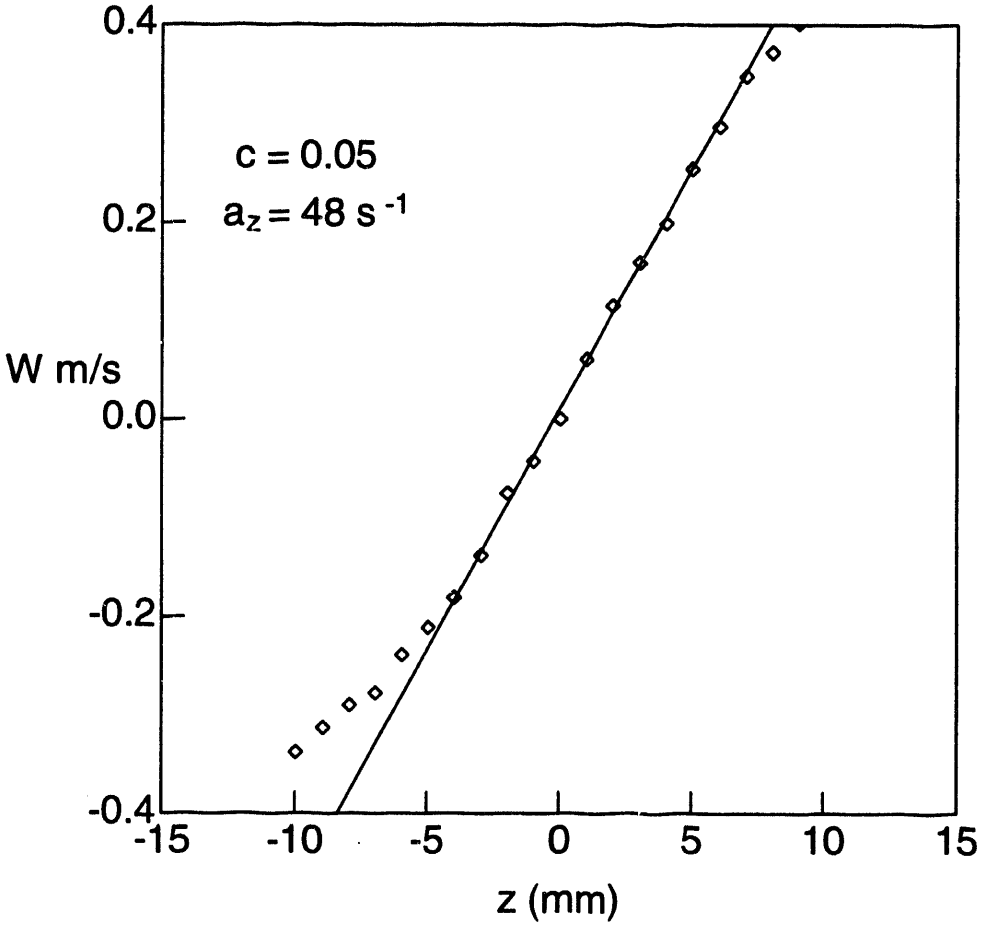
0.4
0.2
0.0
-0.2
-0.4
W m/s
c = 0.05
$a_z = 48\ s^{-1}$
-15
-10
-5
0
5
10
15
z (mm)

DATE FILMED

6/29/94

END